Earth and Planetary Science Letters 494 (2018) 124–134

Contents lists available at ScienceDirect

Earth and Planetary Science Letters

www.elsevier.com/locate/epsl

Precipitation changes over the eastern Bolivian Andes inferred from speleothem ($\delta^{18}O$) records for the last 1400 years

James Apaéstegui [a,b,*], Francisco William Cruz [c], Mathias Vuille [d], Jens Fohlmeister [e,f], Jhan Carlo Espinoza [a], Abdelfettah Sifeddine [g], Nicolas Strikis [h], Jean Loup Guyot [i], Roberto Ventura [j], Hai Cheng [k,l], R. Lawrence Edwards [l]

[a] Instituto Geofísico del Perú, Lima, Peru
[b] Instituto Cientifico del Agua, Pontificia Universidad Católica del Perú, Lima, Peru
[c] Instituto de Geociências, Universidade de São Paulo, São Paulo, Brazil
[d] University at Albany, SUNY, Albany, NY, USA
[e] Institute of Earth and Environmental Science, University of Potsdam, Potsdam, Germany
[f] GFZ German Research Centre for Geosciences, Section 5.2 Climate Dynamics and Landscape Development, Potsdam, Germany
[g] UMR LOCEAN (IRD/UPMC/CNRS/MNHN), Paris-Jussieu, France
[h] Departamento de Geoquimica, Universidade Federal Fluminense, Niterói, RJ, Brazil
[i] UMR GET (IRD) Géosciences Environnement Toulouse, CNRS-IRD-UPS, OMP, Toulouse, France
[j] Instituto de Geociências, Universidade de Brasilia, Brasilia, DF, Brazil
[k] Institute of Global Environmental Change, Xi'an Jiaotong University, Xi'an, China
[l] Department of Geology and Geophysics, University of Minnesota, Twin Cities, Minneapolis, MN, USA

ARTICLE INFO

Article history:
Received 14 February 2017
Received in revised form 7 April 2018
Accepted 24 April 2018
Available online xxxx
Editor: H. Stoll

Keywords:
speleothems
stable isotopes
MCA
LIA
Bolivia
South American Monsoon

ABSTRACT

Here we present high-resolution $\delta^{18}O$ records obtained from speleothems collected in the eastern Bolivian Andes. The stable isotope records are related to the regional- to large-scale atmospheric circulation over South America and allow interpreting changes in $\delta^{18}O$ during the last 1400 yr as a function of changes in precipitation regimes over the southern tropical Andes. Two distinct phases with more negative $\delta^{18}O$ values, interpreted as periods of increased convective activity over the eastern Andean Cordillera in Bolivia are observed concomitantly with periods of global climate anomalies during the last millennium, such as the Medieval Climate Anomaly (MCA) and the Little Ice Age (LIA) respectively. Changes in the Bolivian $\delta^{18}O$ record during the LIA are apparently related to a southward displacement of the Intertropical Convergence Zone (ITCZ), which acts as a main moisture driver to intensify convection over the tropical continent. During the MCA, however, the increased convective activity observed in the Bolivian record is likely the result of a different mechanism, which implies moisture sourced mainly from the southern tropical Atlantic. This interpretation is consistent with paleoclimate records further to the north in the tropical Andes that show progressively drier conditions during this time period, indicating a more northerly position of the ITCZ. The transition period between the MCA and the LIA shows a slight tendency toward increased $\delta^{18}O$ values, indicating weakened convective activity. Our results also reveal a non-stationary anti-phased behavior between the $\delta^{18}O$ reconstructions from Bolivia and northeastern Brazil that confirms a continental-scale east–west teleconnection across South America during the LIA.

1. Introduction

Several studies have revealed that important changes occurred in the mean state of the South American Monsoon System (SAMS) during the last millennium, including the period corresponding to the Medieval Climate Anomaly (MCA, ~900–1100 C.E.) and the Little Ice Age (LIA, ~1500–1850 C.E.) (e.g. Bird et al., 2011; Kanner et al., 2013; Novello et al., 2012, 2016; Vuille et al., 2012; Apaéstegui et al., 2014). Reconstructions based on oxygen isotopes ($\delta^{18}O$) from lacustrine sediments, speleothems and ice core records document that the MCA was characterized by higher values of $\delta^{18}O$, suggesting a weakened SAMS in the Andes. In contrast, the LIA shows opposite conditions with lower $\delta^{18}O$ values that suggest a period of increased SAMS activity (Reuter et al., 2009;

* Corresponding author.
E-mail address: japaestegui@gmail.com (J. Apaéstegui).

https://doi.org/10.1016/j.epsl.2018.04.048
0012-821X/

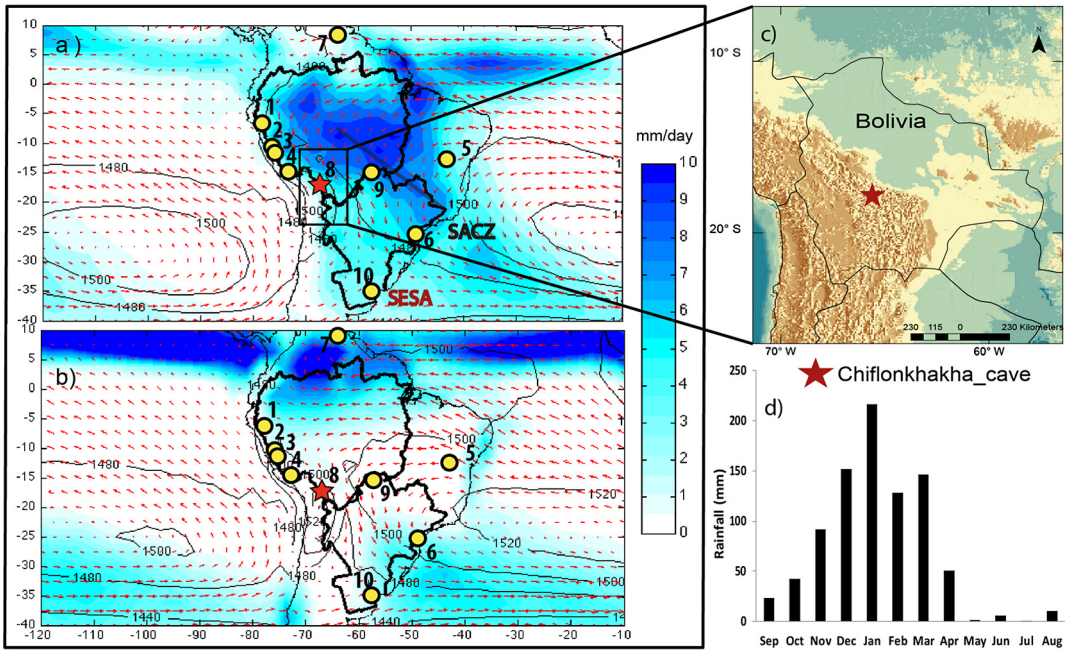

Fig. 1. Geopotential height (contours, in geopotential meters – gpm) and total wind at 850 hPa from ERA-40 for the 1975–2002 period and mean daily rainfall (shading) from CMAP data for the 1979–2002 period. Panel (a) shows DJF season; (b) JJA season. Limits of the Amazon and La Plata basins are shown. The numbers in the Figure indicate locations of SESA – SACZ areas and proxy records in South America: (1) Palestina cave record (Apaéstegui et al., 2014); (2) Pumacocha lake record (Bird et al., 2011); (3) Huagapo cave record (Kanner et al., 2013); (4) Quelccaya Ice Cap (Thompson et al., 2013); (5) DV2 cave record (Novello et al., 2012); (6) Cristal cave record (Vuille et al., 2012); (7) Titanium record from Cariaco Basin (Haug et al., 2001); (8) Bolivian record (this study). (9) Pau d'Alho Cave record (Novello et al., 2016); (10) GeoB 13813-4 record (Perez et al., 2016); Panel (c) shows the location of the Umajalanta–Chiflonkhakha cave system. (d) Monthly mean precipitation recorded at the Torotoro meteorological station (1999–2004).

Bird et al., 2011; Kanner et al., 2013; Vuille et al., 2012; Apaéstegui et al., 2014). These changes in SAMS intensity were associated with displacements of the Intertropical Convergence Zone (ITCZ) to the south during the LIA and to the north during the MCA (Haug et al., 2001).

The regional coherence among isotopic records from the tropical Andes during the LIA indicates a large-scale intensification of the SAMS at that time. During the MCA, however, the magnitude of the isotopic excursion appears to be dependent on latitude with a stronger isotopic signal at lower latitudes ($<10°$S). This north–south gradient seen in the isotopic records during the MCA has been attributed to changes in the winter contribution to total annual precipitation (Apaéstegui et al., 2014). Nevertheless, there is a need for additional paleoclimate reconstructions from the tail end of the SAMS in the southern tropical Andes to compare with more northern records, in particular during the MCA. The lack of records to adequately reconstruct the regional climate response to the radiative forcing anomalies during the LIA and MCA (Bird et al., 2011; Novello et al., 2016) has complicated advancing our understanding of the underlying dynamical mechanisms involved in changing the tropical South American rainfall patterns and the SASM mean state. In order to better document how external forcing affected the SAMS variability and to understand the underlying mechanisms, it is necessary to develop a denser network of proxy records.

The current understanding of climate variability in South America is growing rapidly as discussed in several recent reviews (e.g. Zhou and Lau, 1998; Vera et al., 2006; Garreaud et al., 2009; Marengo et al., 2012). The atmospheric dynamics associated with occurrence of extreme precipitation events in the southwestern Amazon basin and especially over Bolivia were discussed in Espinoza et al. (2014). These events are associated with intense flooding over the southwestern Amazon, while at the same time dry conditions persist in southeastern Brazil, which, in some instances, have led to profound crises in water supply for agriculture, energy production and lack of drinking water and sanitation for the population of the largest cities in Brazil (Coelho et al., 2015). This out of phase relationship between extreme precipitation over the western Amazon and drought over southeastern Brazil has been systematically analyzed for the last three decades by Cavalcanti et al. (2016). Documenting and understanding continental-scale rainfall teleconnections for longer timescales (e.g. over the last millennium), would go a long way in analyzing the proxy network over the South American monsoon region in a dynamically more meaningful and plausible way.

In order to document past precipitation changes along the eastern slope of the southern tropical Andes, we developed stable isotope time series (δ^{18}O) from Bolivian speleothems (65.77°W; 18.12°S, 2650 m.a.s.l.; Fig. 1a). Our site represents the first speleothem record published from Bolivia and it is also the southernmost isotopic record from the tropical Andes. Indeed, it allows exploration of atmospheric teleconnections when compared and synthesized with other regional records in South America. The eastern Bolivian Andes are subject to extreme precipitation seasonality as they are located at the most distal site influenced by the SAMS, where precipitation occurs almost exclusively during the mature phase of the summer monsoon season in November–March (NDJFM; Garreaud et al., 2003).

2. Climatic conditions along the eastern slopes of the southern tropical Andes

The Umajalanta–Chiflonkhakha cave system (65.77 W; 18.12°S; 2650 m.a.s.l.) (Fig. 1c) represents the largest cave system in the Bolivian territory and one of the few locations with occurrence of suitable speleothems for paleoclimate reconstruction. These caves are formed in the cretaceous limestone bank of the "Miraflores" formation located in the Torotoro National Park in the Department of Potosi; a rare example of karst terrain in Bolivia. It is known as the Umajalanta–Chiflonkhakha karst system, extending

underground over an area of several kilometers (Guyot and Soares, 1997). In addition, the Miraflores formation is better known as a source of Cretaceous fossils, including the stromatolite beds much used for lapidary slabs, cubes, eggs and spheres.

Precipitation over the eastern Andes of Bolivia is characterized by a strong spatial gradient, with dry conditions over the highlands (300 mm/yr) and extremely wet conditions (7000 mm/yr) along the eastern flank of the cordillera (e.g. Vuille and Keimig, 2004; Garreaud et al., 2009; Espinoza et al., 2015). The region is further characterized by a strong precipitation seasonality, remaining extremely dry during most of the year except for austral summer (November to March) when intense convective storms bring significant precipitation (Vuille, 1999; Vuille et al., 2000; Garreaud et al., 2003) which corresponds to ∼85% of total annual rainfall (Fig. 1a, b, d). The three months with peak river runoff (JFM) contribute 75% of the annual discharge and deliver up to 90% of the annual sediment transport in the Caine River, which drains the Torotoro basin (Guyot et al., 1994). Seasonal rainfall is the result of the destabilization of the local boundary layer by the intense surface heating and the establishment of upper-level easterly winds (200 hPa) that favor the transport of moist air from the interior of the continent (Vuille, 1999; Garreaud et al., 2003; Falvey and Garreaud, 2005). These upper-air easterlies are the result of the strengthening of the Bolivian High, an upper-level high pressure cell that develops over the central Andes in response to the latent heat release during monsoon-related convection and condensation over the Amazon Basin (Lenters and Cook, 1997; Marengo et al., 2012).

Precipitation over the southwestern Amazon Basin, including the eastern slopes of the Bolivian Andes, occurs in association with low-level (1000–850 hPa) moisture transport from the tropics, but is also related to active and break phases of the South Atlantic Convergence Zone (SACZ) and easterly moisture transport over central South America, perhaps related to the influence of the South American low level jet (Herdies et al., 2002). This interplay generates a precipitation dipole between southeastern South America (SESA) and the SACZ region (Fig. 1a). Dry (wet) conditions over the SACZ region occur when wet (dry) conditions prevail over SESA and in the western Amazon and are related to the anomalous moisture flux over the continent which is directed toward the west (Andes) and south (SESA). The main moisture source for the southern Amazon Basin is located over the tropical Atlantic, including northern and southern sectors (Satyamurty et al., 2013). Nevertheless, moderate to extreme events that are instrumental in forming the precipitation dipole between SESA and the southwestern Amazon (including the eastern Andean slopes of Bolivia) have larger contribution from moisture transported from the South Atlantic rather than from the tropical Atlantic (Espinoza et al., 2014; Coelho et al., 2015; Cavalcanti et al., 2016).

There is a general agreement that a significant fraction of the interannual variability in precipitation over the central Andes is related to the El Niño–Southern Oscillation (ENSO) phenomenon (e.g. Lenters and Cook, 1999; Vuille, 1999; Vuille et al., 2000; Garreaud and Aceituno, 2001; Garreaud et al., 2009). During El Niño (La Niña) less (more) summer precipitation is observed in the eastern Andes and the Altiplano due to weakened (enhanced) upper-level easterly winds aloft, reducing (favoring) moisture influx from the east. In addition, a recent study shows that the dominant forcing associated with decadal-interdecadal rainfall variability over the Andes–Amazon transition region appears to be related to low-frequency SST variability of the central tropical Pacific and 200 hPa winds aloft (Segura et al., 2016).

The importance of the meridional SST gradient between the tropical and subtropical South Atlantic as major driver of moisture transport from the Atlantic toward the southwestern Amazon has also been documented (Ronchail et al., 2005; Yoon and Zeng, 2010; Lavado et al., 2012). For instance, during the summer of 2014, the exceptionally warm subtropical Atlantic, aided by warm conditions in the western Pacific/eastern Indian Ocean, triggered abundant rainfall and flooding over the southwestern Amazon (Espinoza et al., 2014). On decadal and longer timescales, there is a lack of studies documenting climate variability in the Andes, because of limited instrumental data. Nevertheless, paleoclimate reconstructions all point to the Atlantic as playing an important role for modulating precipitation variability at decadal and multidecadal timescales over the tropical Andes (Baker et al., 2005; Bird et al., 2011; Vuille et al., 2012; Apaéstegui et al., 2014). The inter-hemispheric SST gradient in the Atlantic regulates latitudinal shifts of the ITCZ, which in turn determines moisture influx over tropical South America at multiple time scales (Haug et al., 2001).

3. δ^{18}O variability in the Bolivian Andes

Isotopic variability in precipitation over the eastern central Andes has been the subject of several recent studies. Local and regional influences on isotope fractionation of precipitation in the Bolivian Andes have been discussed and interpreted in order to determine the climatic controls on the isotopic signature of precipitation (Vimeux et al., 2005; Insel et al., 2013; Fiorella et al., 2015). Local rainout is insufficient to explain isotopic variations at seasonal timescales. Moreover, Amazon distillation of air masses over the Amazon can explain up to 90% of δ^{18}O and δD variance in rainfall along the Zongo Valley in Bolivia (Vimeux et al., 2005; Vuille and Werner, 2005). An evaluation of the δ^{18}O signature in precipitation along the Andes based on a regional isotope model (REMOiso) (Sturm et al., 2008) reveals that variability in oxygen isotope ratios for the central eastern Andean region (10°S–30°S) is governed by the amount effect and wind trajectories, which are related to the easterly winds anomalies in the upper troposphere modulated by the position of the Bolivian High (Insel et al., 2013). Fiorella et al. (2015) revisited the climatic controls on oxygen isotopes in precipitation and confirmed that interannual variability in δ^{18}O is tied to continental-scale climate dynamics and upwind precipitation anomalies, which appear to have a dominant effect on the isotopic signal. In fact, interannual δ^{18}O variability is largely consistent with precipitation anomalies over major air sourcing regions, supporting the idea that remote and upstream precipitation amount anomalies are preserved in and provide a primary control on central Andes δ^{18}O variability (Samuels-Crow et al., 2014; Fiorella et al., 2015; Hurley et al., 2016).

Based on this evidence, we interpret δ^{18}O in precipitation over the eastern Andes of Bolivia as being mainly related to rainfall intensity upstream during the austral summer SAMS season. The modern annual mean precipitation-weighted value of δ^{18}O for our study region, based on spatially interpolated isotope observations from the Global Network of Isotopes in Precipitation (GNIP), is $\sim -13.1‰ \pm 0.7$ (95% confidence interval). Uncertainties and methods related to the spatial interpolation are provided in Bowen and Revenaugh (2003) and the Online Isotopes Precipitation Calculator (http://wateriso.utah.edu/waterisotopes/pages/data_access/oipc.html). This annual mean value is the result of different moisture sources that contribute to regional precipitation to varying degrees on intraseasonal and interannual time scales. The cluster means analyses for the back trajectory winds at the study region reveal four principal moisture source regions (Fig. S1), with the principal regions being located in the North and South Atlantic, respectively. These moisture sources depend on the location and intensity of the Bolivian High and related upstream precipitation anomalies during the SAMS season (Fiorella et al., 2015).

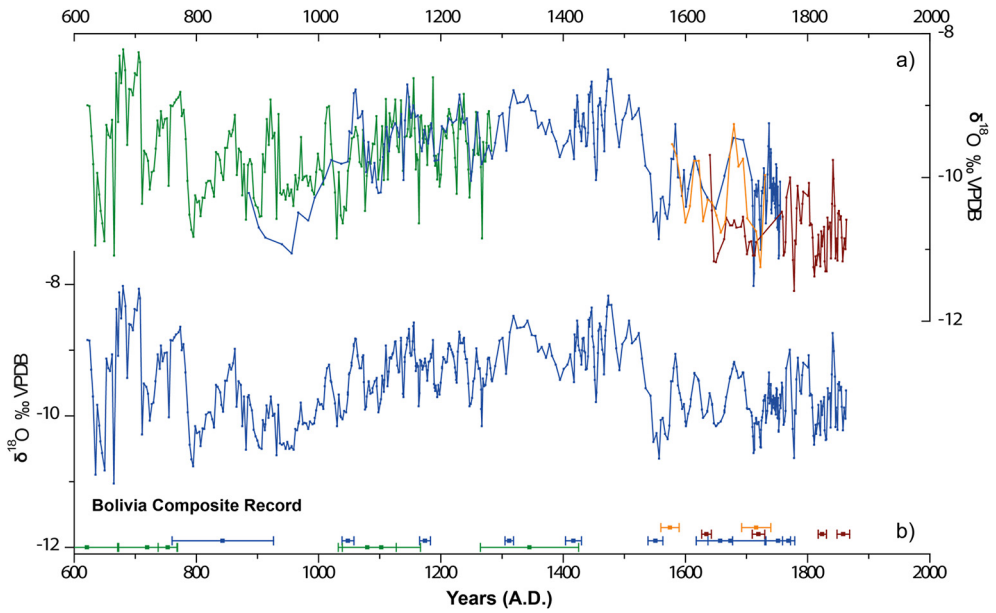

Fig. 2. a) Stable isotope (δ^{18}O) time series obtained from linear interpolation between dates for Boto3 (blue line), Boto7 (brown line), Boto10 (green line), and Boto1 (orange line) respectively. U–Th dates and corresponding error bars are represented by blue, brown green and orange dots for Boto3, Boto7, Boto10 and Boto1 stalagmites, respectively. b) Bolivia composite record reproduced by the ISCAM models after age modeling adjustments of each speleothem record in the composite record. (For interpretation of the colors in the figure(s), the reader is referred to the web version of this article.)

4. Materials and methods

Four speleothems were collected in May 2010 from the Umajalanta–Chiflonkhakha cave system, hereafter referred to as Boto1, Boto3, Boto7 and Boto10. Speleothem Boto1 is a 85.3 cm long stalagmite deposited in the first chamber of the Chiflonkhakha cave, at ∼200 m from the entrance. Unfortunately the topmost interval of the sample Boto1 presented high concentration of detrital Th, which precluded a precise dating. Only the section of the sample, corresponding to the interval between 72 and 115 mm, was considered for this study. Boto3 is a 7.5 cm tall stalagmite collected at 300 m distance from the Chiflonkhakha cave entrance. There is no evidence of recent carbonate deposition although the sample surface was underneath active dripping at the time of collection. Boto7 is a 13 cm tall stalagmite collected at 70 m distance from where the Boto3 sample was taken (∼370 m from the cave entrance). The Boto10 stalagmite is 12 cm tall and was collected at 400 m distance from the Umajalanta cave entrance. All samples were dated by U–Th method, using an inductively coupled plasma-mass spectrometry (ICP-MS) technique (Cheng et al., 2013a) at the University of Minnesota isotope laboratory. A preliminary chronological age model was developed for each speleothem by linear interpolation of dated depths (Fig. S2).

Samples for oxygen isotope analysis were collected continuously along the stalagmite growth axis at intervals varying from 0.1 to 1.5 mm. Sampling resolutions were calculated in dependence of the sample growth rate with the intention of obtaining a time resolution equivalent to ∼3 yr. Oxygen isotope measurements were performed on a Delta Plus Advantage (Thermo Finnigan) mass spectrometer in the "Laboratorio de Estudos Geodinâmicos e Ambientais" at the University of Brasilia (UnB), Brazil. The standard deviation for δ^{18}O analyses is 0.1‰. Oxygen isotope records are reported relative to the Vienna PDB Standard.

A statistical approach to construct composite records (*iscam*, Fohlmeister, 2012) was then applied to finalize the age models for the individual records (Boto1, Boto3, Boto7 and Boto10; Fig. 2a). This age-depth modeling software uses a Monte-Carlo approach on absolute age determinations to find the best correlation between climate proxies of several signals reproducing adjacent archives (Fig. 2b). Age uncertainties at 68%, 95% and 99% significance levels are obtained from evaluation of a set of 2000 first order autoregressive processes (AR1) for each record, which have the same statistical characteristics as the individual records. This method allows significantly reducing the age uncertainty within the overlapping periods and it can be tested if the signal of interest is indeed similar in all the records (Fohlmeister, 2012). The chronological age-depth relationship in the overlapping parts of the individual stalagmites was modified and improved according to the *iscam* results of the composite record (Table S1, Figs. S5, S6).

The composite record is evaluated by applying a Hubert segmentation test in order to determine breaks in the data (Hubert et al., 1989). The segmentation procedure is a sort of a stationarity-test. Based on a study of the "break" observed in the isotope series, it is possible to determine whether or not a time series is homogeneous (stationary) and, if not, determine as many homogeneous sub-series as possible. Spectral analysis techniques were performed on annually interpolated time series and wavelet analysis was used to display the time-dependent changes in dominant frequency bands in the δ^{18}O time series (Torrence and Compo, 1998) (Fig. S7).

5. Results

Speleothem growth periods were determined based on 22 U/Th dates with 2σ-errors typically <1% (Table S5). The segment analyzed from the Boto1 sample spans the period between ∼1575 and 1716 C.E. Sample Boto3 was formed during the period between ∼844 and 1770 C.E. (10 U/Th dates). There is no evidence of long hiatuses according to the approximately uniform distribution of U/Th dates, despite the visible discontinuities identified along its growth axis (Fig. S2). Nevertheless, the record is well complemented by the segment of Boto7 between 2 and 40 mm, which grew during the period from ∼1635 to 1859 C.E. (4 U/Th dates), and Boto10, which covers the period from ∼622 to 1346 C.E. (6 U/Th dates) (Table S5). In general, combining the four speleothems allows establishing a continuous record covering most of the last 1400 yr (Fig. 2, S7). Overlapping segments

between samples further allow replicating information during several growth periods.

The four speleothems co-vary and present a similar range of $\delta^{18}O$ values during periods of overlap (Fig. 2a), which suggests that common climatic factors govern their isotopic signal. Since there is a good correspondence between $\delta^{18}O$ values in all the samples, a unique composite record was constructed using the *iscam* model (Fohlmeister, 2012) and named Bolivian composite record. (Fig. 2b). The combined stable isotope time series ($\delta^{18}O$) is composed of 575 measurements and provides an average temporal resolution of ~2 yr spanning most of the last 1400 yr.

The $\delta^{18}O$ record is dominated by variability at decadal and centennial timescales with a range in the order of ~3‰ over the entire record (Fig. S7). REDFIT (Schulz and Mudelsee, 2002) spectral analyses show strong periodicities at 85, 50 and 30 yr exceeding the 95% significance level (Fig. S7). The Hubert segmentation test identifies seven break points in the time series that allow separation of eight intervals during the record (significant at $p < 0.01$, Scheffé significance test, Hubert et al., 1989). During the period ~620 to 668 C.E. $\delta^{18}O$ values are on the order of −10‰, before they rapidly switch to more enriched values during the period ~669–710 C.E. (−8.7‰). From ~711 to 734 C.E. the $\delta^{18}O$ time series experiences rapid change toward more negative values of −10.6‰ (average −9.86‰). Between ~735 and 784 C.E. the $\delta^{18}O$ values increase to −9.2‰. The period between ~785 and 1049 C.E. shows mean values of −10.1‰ with a peak value of −9.1‰ centered at ~862 C.E. From ~1050 to 1292 C.E. the $\delta^{18}O$ time series reveals a slight trend toward more positive values (average −9.4‰) with a muted amplitude on the order of ~1‰. The period between ~1293 and 1532 C.E. maintains the positive trend observed in the previous period showing average values of −9‰. Afterwards an abrupt shift of −1.7‰ occurs, resulting in values of −10.7‰ at ~1553 C.E. The most recent period after ~1553 C.E. features high variability, with significant excursions in $\delta^{18}O$ on the order of ~−1‰ (Figs. 2, S7a).

6. Discussion

Independent chronological measurements performed for the Bolivian speleothems reveal that the samples grew over different time intervals. However, samples are complementary and contain overlapping periods that cover most of the last 1400 yr (Fig. 2). It is important to note that even though samples have independent chronological models, stable isotopes measured in the Bolivian speleothems co-vary and cover a similar range of $\delta^{18}O$ values. $\delta^{18}O$ and $\delta^{13}C$, sampled along the growth axis (Fig. S3), are significantly correlated in the Boto1, Boto3 and Boto10 samples ($r = 0.55$; 0.50 and 0.55, $p < 0.01$, respectively) while low correlation exists in Boto7 ($r = 0.23$, $p < 0.05$). Although these results suggest that the isotope fractionation between drip water and calcite during speleothem formation may not be in isotopic equilibrium, it is unlikely that kinetic fractionation effects could disrupt the link between $\delta^{18}O$ and precipitation variability. In fact the variations in $\delta^{18}O$ are first and foremost related to climatic variability as indicated by very good replication of the $\delta^{18}O$ signal amongst different speleothem samples. Indeed, a dominant kinetic fractionation process is site specific and tends to produce heterogeneous variations in coeval isotope records (Hendy, 1971).

While the IPCC defines the MCA and LIA as periods that span the time 950–1250 C.E. and 1450–1850 C.E. respectively (Masson-Delmotte et al., 2013), the timing of these events is quite variable in South American records. (e.g. Bird et al., 2011; Kanner et al., 2013; Novello et al., 2012, 2016; Vuille et al., 2012; Apaéstegui et al., 2014). Based on the isotopic variations seen in the Bolivian record, we here define the MCA and LIA as periods that span the time intervals 900–1100 C.E. and 1500–1850 C.E., respectively. Both of these time periods fall within the boundaries as defined by the IPCC (Masson-Delmotte et al., 2013) based on global records. We also analyze changes during the transition period (1100–1500 C.E.) to characterize how climate transitioned from MCA to LIA based on the observations from our proxy record (Table S3).

The Bolivian record reveals both similarities and differences when compared with other $\delta^{18}O$ reconstructions along the eastern Andes (Fig. 3). During the period between ~785 and 1049 C.E., corresponding to the MCA, the Bolivian record is characterized by more negative $\delta^{18}O$ values (Fig. 3e), in contrast to the northern Andean records that show positive $\delta^{18}O$ anomalies related to a weakened SAMS (Fig. 3a, b, c, d) (Bird et al., 2011; Vuille et al., 2012; Apaéstegui et al., 2014). In fact, the isotopic expression of the MCA drought, seen in the northern tropical Andes, becomes progressively weaker the farther south the proxies are located, until ultimately this dry excursion is no longer detectable in the Bolivian region. Hence, it appears that the MCA was anomalously wet in Bolivia, at least in a regional context (Table S3, Fig. S8). The more negative $\delta^{18}O$ values during the LIA in our Bolivian record, however, are consistent with other Andean records that suggest increased SAMS activity at that time (Reuter et al., 2009; Bird et al., 2011; Vuille et al., 2012; Kanner et al., 2013; Thompson et al., 2013; Apaéstegui et al., 2014). The onset of the LIA period, however, occurs around 180 yr later than in other Andean records and is characterized by an abrupt change in the $\delta^{18}O$ values (~1.7‰), not evident in any other record (Fig. 3e).

Lacustrine records from the Andean region, such as diatom assemblages in Lake Titicaca (Tapia et al., 2003) and isotope records in Lake Umayo (Baker et al., 2005) reveal similar trends as the Bolivian composite record (Fig. 3g). Despite the lower resolution, the Lake Umayo isotope record also shows lower $\delta^{18}O$ values between ~800 and 1000 C.E., which is interpreted as reflecting an intensification in the pluvial regime over the lake. Despite chronological uncertainties, the increase in fresh water diatoms from Lake Titicaca observed at around 1000 C.E. can be related to increased precipitation as inferred from the Bolivian composite record during the MCA (Fig. 3f). Nevertheless, lake records do not show a contemporaneous period of increased precipitation during the LIA as expected, but chronological uncertainties of these lacustrine records are large.

In order to explain the observed differences in the Andean isotope records during the MCA period, it is necessary to consider the latitudinal location of the proxies analyzed and the changes in the moisture source for the different regions. Low latitude records (north of 10°S) receive a relatively high proportion or rainfall outside of the main wet season (Espinoza et al., 2009); hence their isotopic signal could be more strongly biased by a varying contribution of austral winter rainfall (Apaéstegui et al., 2014). On the other hand, the Bolivian site receives precipitation almost exclusively during the core monsoon season and changes in seasonality are unlikely to have significantly affected this region over the past millennium. Alternatively, the moisture source of the rainfall in the Bolivian Andes may have changed during the MCA.

Paleo-precipitation reconstructions based on speleothem $\delta^{18}O$ records from southeastern and central Brazil have shown evidence for diminished precipitation during the MCA (Vuille et al., 2012; Novello et al., 2016), (Fig. 4a, b). For the same period, humid conditions have been reported from lake records in northeastern Argentina (Piovano et al., 2009) and from fresh water diatoms, deposited offshore by sediments from the La Plata river (Perez et al., 2016; Fig. 4d). These opposite conditions are consistent with the notion of an active precipitation dipole between SACZ and SESA regions during the MCA, likely extending northwestward toward the Bolivian region (Fig. 4c). During the LIA, on the other hand, the intensification of the SAMS is coherent among all records and con-

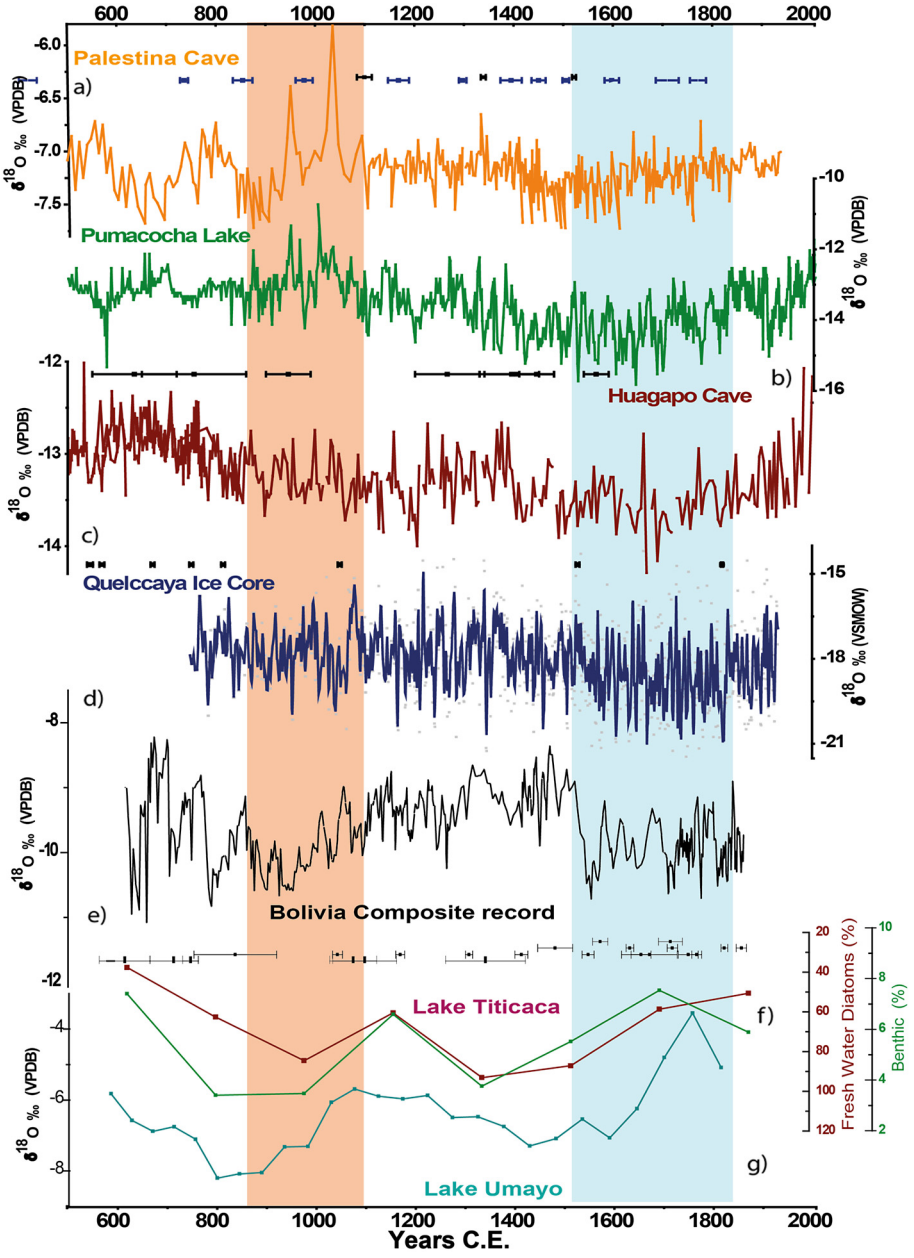

Fig. 3. Comparison between (e) Bolivian composite record (black line) and other eastern Andean records with their respective chronological controls and error bars. From top to bottom: (a) Palestina record (Apaéstegui et al., 2014); (b) Pumacocha lake record (Bird et al., 2011); (c) Huagapo cave record (Kanner et al., 2013); (d) Quelccaya Ice Cap (Thompson et al., 2013); (f) Lake Titicaca assemblage for fresh water (red) and benthic (green) diatoms; (g) Lake Umayo isotope record (Baker et al., 2005); Shaded background represents MCA (red) and LIA periods (light blue).

firms the region-wide signal observed previously throughout the tropical Andean region.

Modern observations of western Amazon precipitation show contrasting interannual evolution of wet day frequency (WDF) and dry day frequency (DDF) in the northern and southern Amazon basin (Espinoza et al., 2016). This feature reveals increased WDF in the northern region since 1995 and contrasting increased DDF in the southern region, including an increasing dry season length in the southern Amazon basin (Fu et al., 2013), which implies a trend to opposite conditions in the northern and southwestern Amazon. Indeed, the concurrence of extreme precipitation events over the western Amazon with droughts in southeastern Brazil has been documented in the literature (Coelho et al., 2015; Cavalcanti et al., 2016). This dipole pattern has been associated with anomalously warm conditions in the western tropical Pacific–eastern Indian Ocean and an exceptionally warm subtropical South Atlantic (Ronchail et al., 2005; Espinoza et al., 2014; Coelho et al., 2015; Cavalcanti et al., 2016).

There is evidence of higher temperatures in the Indo-Pacific region during the MCA, when compared to present-day (Oppo et al., 2009, Fig. 4e), but to what extent this might have triggered extratropical wave propagation influencing precipitation along the eastern Bolivian Andes is not well investigated. Hurley et al. (2015) recently documented a major role for extra-tropical Rossby waves and cold air incursions in triggering major snowfall events during austral summer in the eastern Andes of southern Peru. Another potential source of moisture that might affect the Bolivian Andes–Amazon transition, but not areas further north, is associated with the tropical–subtropical South Atlantic SST gradient (Espinoza et al., 2014; Cavalcanti et al., 2016). Unfortunately, there is a lack of proxy evidence documenting SST changes in the South Atlantic at high resolution for the last millennium. Hence the role of this SST

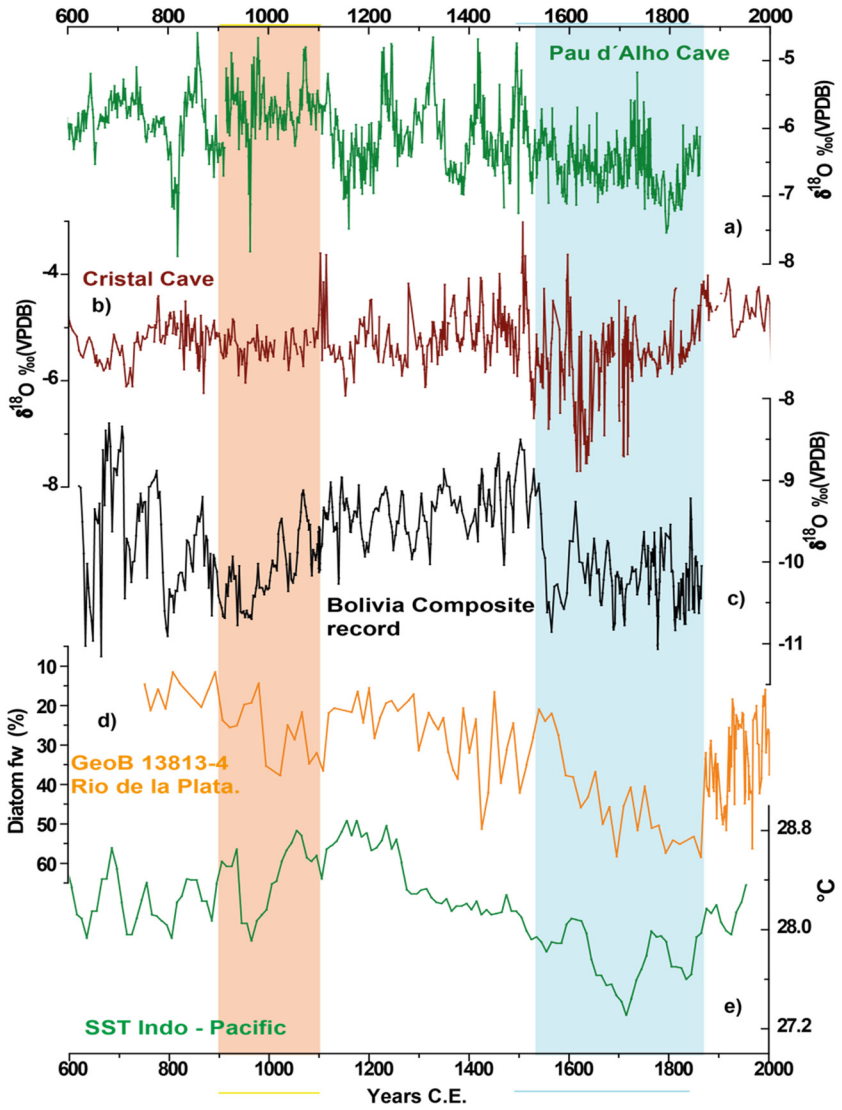

Fig. 4. Comparison between (c) Bolivian composite record (black line) and other South American records. From top to bottom: (a) Pau d'Alho cave record (Novello et al., 2016); (b) Cristal cave record (Vuille et al., 2012); (d) Fresh water diatom percentage in sediments of La Plata river basin (Perez et al., 2016); (e) Sea surface temperature reconstructions from foraminifera in the Indo-Pacific region (Oppo et al., 2009); Shaded background represents MCA (red) and LIA periods (light blue).

gradient in delivering moisture to the southernmost part of the tropical Andes remains somewhat elusive on paleoclimatic time scales and will require more attention in the future from both the proxy and modeling community.

A comparison with other records of the SAMS, which are not located in the Andean region, shows consistent features, which are also observed in the Bolivian $\delta^{18}O$ record. Most notably, the negative excursion during the LIA solidifies key elements that characterize a coherent history of the SAMS over the last millennium (Vuille et al., 2012). An important new aspect of our record is the anti-phasing with the $\delta^{18}O$ record from northeastern Brazil (Novello et al., 2012) (Fig. 5b, c). The significant negative correlation between the two records interpolated to equivalent resolutions of 5, 10, 20, 30, 40 and 50 yr ($-0.5 \leq r \leq -0.37$, $p < 0.001$; Table S4, Fig. S9) suggest that both areas of South America are influenced by the SAMS, albeit with opposite hydro-climatologic results. Running average correlation using a 50-yr window between the Bolivia composite and the DV2 record indicates a non-stationary relationship (Fig. S10). The anti-phasing in precipitation between northeastern Brazil and most of the rest of tropical South America has been observed and documented in modern climate (Sulca et al., 2016), on centennial (Novello et al., 2012), as well as on orbital time scales (Cruz et al., 2009; Cheng et al., 2013b). This precipitation dipole results from enhanced monsoon activity and release of latent heat during strong convective activity over the Amazon and Congo basins, which in turn intensifies the Bolivian High–Nordeste low system (Lenters and Cook, 1997; Chen et al., 1999; Liu and Battisti, 2015). During periods of enhanced SAMS activity the intensified convection and upward motion over the core monsoon region is balanced by increased upper-level convergence and subsidence, which results in a deficit in summer precipitation over northeastern Brazil (Novello et al., 2012). Our records from Bolivia and NE Brazil confirm this anti-phased behavior between the two sites throughout the LIA period.

Although an antiphased behavior in the isotopic signals between both regions persist during the MCA it is unlikely to be related to the same mechanism, since the strength of the SAMS was diminished during that period (Vuille et al., 2012). Instead, the antiphased behavior is most probably the result of a northward migration of the ITCZ which in turn diminished precipitation in NE Brazil, reduced the monsoon strength over the northern and central tropical Andes, while the Bolivian site at the southernmost tail end of the monsoon region must have received more moisture from a different source. This explanation is supported by atmo-

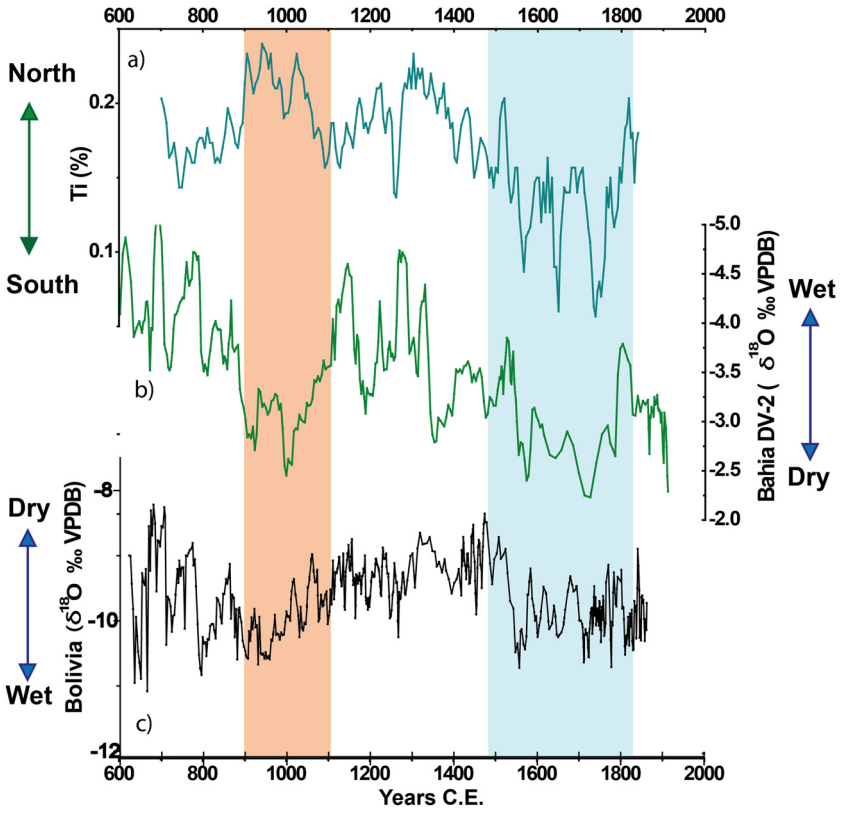

Fig. 5. Comparison between the Bolivian composite record in c) and Ti% record in Cariaco Basin (a) indicating northern and southern location of the ITCZ. (b) Bahia DV-2 stable isotope record (y-axis inverted).

spheric circulation patterns, which can be observed at present-day (Coelho et al., 2015).

Several publications have related periods of SAMS intensification to North Atlantic climate variations and the latitudinal position of the ITCZ (Bird et al., 2011; Vuille et al., 2012; Apaéstegui et al., 2014). It has been demonstrated that during the LIA the ITCZ reached a more southerly position (Fig. 5a) (Haug et al., 2001), which enhanced moisture influx into the SAMS region. This mechanism has been invoked to explain the increased SAMS precipitation as inferred from a number of isotopic proxies in the Andes (Reuter et al., 2009; Bird et al., 2011; Kanner et al., 2013; Apaéstegui et al., 2014), southeastern Brazil (Vuille et al., 2012) and the resulting drier than normal conditions over northeastern Brazil (Novello et al., 2012).

During the MCA on the other hand, the general consensus is that the Atlantic ITCZ remained in a more northerly position (Fig. 5a) (Haug et al., 2001), which in turn diminished the moisture transport to the Amazon basin, weakening the SAMS. Proxy records from the northern tropical Andes are consistent with this hypothesis as they generally show slightly increased $\delta^{18}O$ values, suggesting diminished SAMS activity at this time. Nevertheless, this characteristic during the MCA becomes less evident in the more southern records, suggesting that this reduced SAMS activity was more prevalent over the northern Andes (Table S3, Fig. S8). Such a scenario, however, fundamentally implies another pathway for moisture being transported to the Andes through the southwestern Amazon or through extratropical cold air incursions propagating northward east of the Andes toward low latitudes and triggering precipitation along their leading front (Hurley et al., 2015). Since the anomalously northern position of the ITCZ precludes a significant influence of the tropical North Atlantic as a major source for enhanced moisture transport to the Bolivian Andes, the southern tropical Atlantic was likely the main moisture source region, which could have contributed to the enhanced precipitation at our site during the MCA, with cold air incursions providing the dynamical forcing to destabilize the boundary layer and inducing convection.

In order to clarify our findings, schematic scenarios based on paleoclimate reconstructions for the MCA and the LIA periods are presented (Fig. 6). Contrasting behavior in precipitation is highlighted in order to characterize the precipitation patterns in South America during the MCA and LIA. During the MCA an increase in precipitation is observed in the southern region of the tropical Andes propagating southeast toward the La Plata basin, indicative of increased precipitation in the SESA region (Boers et al., 2014). This circulation pattern is also observed systematically on intraseasonal to interannual timescales when increased precipitation events are recorded in the western–southwestern Amazon (Espinoza et al., 2014; Coelho et al., 2015; Cavalcanti et al., 2016) and could serve as a plausible mechanism to explain changes in the SAMS over the last millennium. During the LIA, however, the precipitation pattern is clearly representing a regional intensification of the SAMS. The proposed scenarios should be verified with model results and more paleoclimate reconstructions in order to further clarify regional aspects of SAMS dynamics.

7. Conclusions

The Bolivian record reveals insightful new information regarding changes in the SAMS during the last millennium, in particular during the MCA period. The anomalously wet conditions during the MCA as revealed in our Bolivian record are in contrast to the drying observed in northern Andean records at that time. Observed differences could be related to changing moisture source contributions, as the ITCZ was likely located at a more northerly position, allowing enhanced moisture influx to the eastern Bolivian Andes from the South Atlantic region. The rainfall in the Bolivian Andes is influenced by moisture influx from this Atlantic region in the modern period (Ronchail et al., 2005), most likely forced

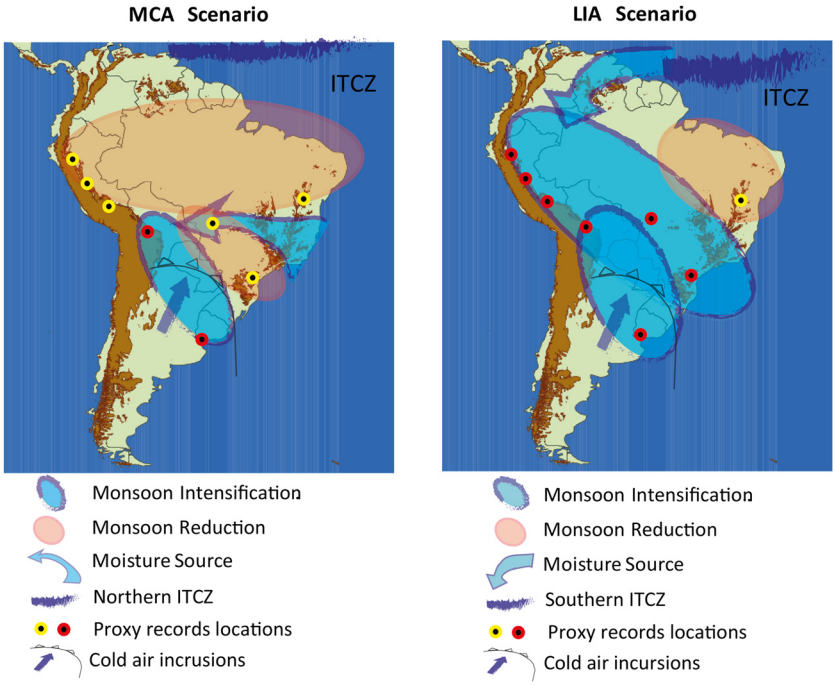

Fig. 6. Schematic representation of precipitation patterns during the MCA and LIA based on paleoclimate reconstructions in South America.

by extratropical wave trains that originate over the Indo-Pacific, and propagate northward east of the Andes toward lower latitudes as cold air masses, producing extremely heavy rain events along their leading edge (Espinoza et al., 2014; Coelho et al., 2015; Hurely et al., 2015). This scenario is consistent with other paleoclimate reconstructions and models that show anomalous heating in the Indo-Pacific region during the MCA (Oppo et al., 2009; Graham et al., 2010). The LIA on the other hand, is characterized by increased SAMS activity in all records of the Andean region, consistent with our Bolivian site.

The Bolivian record further documents teleconnections with precipitation over northeastern Brazil during the last 1400 yr. Although this opposite relationship in precipitation is non-stationary, there is evidence for a significant teleconnection during the LIA period, fueled by increased SAMS activity. The same precipitation dipole can also be observed during the MCA, but it is not the result of a dynamic teleconnection between the two sites, as the precipitation anomalies have distinctly different dynamic origins over the two regions. Hence atmospheric teleconnections modulating precipitation at both sites were non-stationary over the last millennium and do not appear to respond linearly to ITCZ migration or changes in SAMS intensity.

Many aspects of the SAMS system and its variability over the last millennium remain poorly understood, in particular related to the role of the tropical South Atlantic. Sustained efforts are required to improve paleoclimate reconstructions from this region in order to better comprehend its contribution to SAMS variability on a range of time scales.

Acknowledgements

We thank Luis Mancini and Ana Carolina Miranda for their support during the stable isotope data acquisition at the Universidade de Brasília and Osmar Antunes for his support at the Universidade de São Paulo. We also thank Angela Ampuero, Omar Gutierrez and Jairo Valdivia for their computational support. Thanks to Augusto Auler for his support during the fieldwork. This study was undertaken as part of the PALEOTRACES project (IRD-UFF-UANTOF), SOHYBAM and PRIMO cooperative project (CNPq-IRD), and supported by the Fundação de Amparo a Pesquisa do Estado de São Paulo, Brazil (FAPESP grants 2011/39450394 and NASA/FAPESP through the Dimensions of Biodiversity Program grants 2012/50260-6 and 2013/50297-0 to F.W. Cruz) and also by grants 2013CB955902, CNSF 41230524, US NSF grant 0502535 and 3961103404 to L. Edwards and H. Cheng, and NSF grants 1303828, 1523288 and 1743738 to M. Vuille and DFG grant FO809/4-1 to J. Fohlmeister. J. Apaéstegui and JC. Espinoza were partially funded by PNICP-Peru through the 'N397-PNICP-PIAP-2014' contract.

Appendix A. Supplementary material

Supplementary material related to this article can be found online at https://doi.org/10.1016/j.epsl.2018.04.048.

References

Apaéstegui, J., Cruz, F.W., Sifeddine, A., Vuille, M., Espinoza, J.C., Guyot, J.L., Khodri, M., Strikis, N., Santos, R.V., Cheng, H., Edwards, L., Carvalho, E., Santini, W., 2014. Hydroclimate variability of the northwestern Amazon Basin near the Andean foothills of Peru related to the South American Monsoon System during the last 1600 years. Clim. Past 10, 1967–1981. https://doi.org/10.5194/cp-10-1967-2014.

Baker, P.A., Fritz, S.C., Garland, J., Ekdahl, E., 2005. Holocene hydrologic variation at Lake Titicaca, Bolivia/Peru, and its relationship to North Atlantic climate variation. J. Quat. Sci. 20 (7–8), 655–662. https://doi.org/10.1002/jqs.987.

Bird, B.W., Abbott, M.B., Vuille, M., Rodbell, D.T., Stansell, N.D., Rosenmeier, M.F., 2011. A 2300-year-long annually resolved record of the South American summer monsoon from the Peruvian Andes. Proc. Natl. Acad. Sci. 108, 8583–8588.

Boers, N., Bookhagen, B., Barbosa, H.M.J., Marwan, N., Kurths, J., Marengo, J.A., 2014. Prediction of extreme floods in the eastern Central Andes based on a complex networks approach. Nat. Commun. 5, 5199. https://doi.org/10.1038/ncomms6199.

Bowen, G.J., Revenaugh, J., 2003. Interpolating the isotopic composition of modern meteoric precipitation. Water Resour. Res. 39, 1299–1312. https://doi.org/10.1029/2003WR002086.

Cavalcanti Fonseca, I. de A., Marengo, J.A., Alves, M., Filipe, D., 2016. On the opposite relation between extreme precipitation over west Amazon and southeastern Brazil: observations and model simulations. Int. J. Climatol. https://doi.org/10.1002/joc.4942.

Chen, T.-S., Weng, S.-P., Schubert, S., 1999. Maintenance of austral summertime upper-tropospheric circulation over tropical South America: the Bolivian high–Nordeste low system. J. Atmos. Sci. 56, 2081–2100.

Cheng, H., Edwards, L.R., Shen, C.-C., Polyak, V.J., Asmerom, Y., Woodhead, J., Hellstrom, J., Wang, Y., Kong, X., Spötl, C., Wang, X., Alexander, E.C. Jr., 2013a. Im-

provements in ^{230}Th dating, ^{230}Th and ^{234}U half-life values, and U–Th isotopic measurements by multi-collector inductively coupled plasma mass spectrometry. Earth Planet. Sci. Lett. 371–372, 82–91. https://doi.org/10.1016/j.epsl.2013.04.006.

Cheng, H., Sinha, A., Cruz, F.W., Wang, X., Edwards, R.L., d'Horta, F.M., Ribas, C.C., Vuille, M., Stott, L.D., Auler, A.S., 2013b. Climate change patterns in Amazonia and biodiversity. Nat. Commun. 4, 1411.

Coelho, C.A.S., Prestrelo, C., Tércio, D.O., Michelle, A., Reboita, S., Bertoletti, C., José, C., Pereira, L., Campos, S., Carolina, A., Tomaziello, N., Albertani, L., Maria, P., Custódio, D.S., Marcia, L., Dutra, M., Da, R.P., 2015. The 2014 southeast Brazil austral summer drought: regional scale mechanisms and teleconnections. Clim. Dyn. https://doi.org/10.1007/s00382-015-2800-1.

Cruz, F.W., Vuille, M., Burns, S.J., Wang, X., Cheng, H., Werner, M., Edwards, R.L., Karmann, I., Auler, A.S., Nguyen, H., 2009. Orbitally driven east–west antiphasing of South American precipitation. Nat. Geosci. 2 (3), 210–214. https://doi.org/10.1038/ngeo444.

Espinoza, J.C., Ronchail, J., Guyot, J.L., Cocheneau, G., Filizola, N., Lavado, W., de Oliveira, E., Pombosa, R., Vauchel, P., 2009. Spatio-temporal rainfall variability in the Amazon Basin Countries (Brazil, Peru, Bolivia, Colombia and Ecuador). Int. J. Climatol. 29, 1574–1594.

Espinoza, J.C., Segura, H., Ronchail, J., Drapeau, G., Gutierrez-Cori, O., 2016. Evolution of wet- and dry-day frequency in the western Amazon basin: relationship with atmospheric circulation and impacts on vegetation. Water Resour. Res. https://doi.org/10.1002/2016WR019305.

Espinoza, J.C., Marengo, J.A., Ronchail, J., Carpio, J.M., Flores, L.N., Guyot, J.L., 2014. The extreme 2014 flood in south-western Amazon basin: the role of tropical–subtropical South Atlantic SST gradient. Environ. Res. Lett. https://doi.org/10.1088/1748-9326/9/12/124007.

Espinoza, J.C., Chavez, S., Ronchail, J., Junquas, C., Takahashi, K., Lavado, W., 2015. Rainfall hotspots over the southern tropical Andes: spatial distribution, rainfall intensity and relations with large-scale atmospheric circulation. Water Resour. Res. 51. https://doi.org/10.1002/2014WR016273.

Falvey, M., Garreaud, R., 2005. Moisture variability over the South American Altiplano during the SALLJEX observing season. J. Geophys. Res. 110, D22105. https://doi.org/10.1029/2005JD006152.

Fiorella, R.P., Poulsen, C.J., Zolá, R.S.P., Barnes, J.B., Tabor, C.R., Ehlers, T.A., 2015. Spatiotemporal variability of modern precipitation δ^{18}O in the central Andes and implications for paleoclimate and paleoaltimetry estimates. J. Geophys. Res., 4630–4656. https://doi.org/10.1002/2014JD022893.

Fohlmeister, J., 2012. A statistical approach to construct composite climate records of dated archives. Quat. Geochronol. 14, 48–56. https://doi.org/10.1016/j.quageo.2012.06.007.

Fu, R., Yin, L., Li, W., Arias, P., Dickinson, R., Huang, L., Chakraborti, S., Fernandes, K., Liebman, B., Fisher, R., Myneni, R.B., et al., 2013. Increased dry-season length over southern Amazonia in recent decades and its implication for future climate projection. Proc. Natl. Acad. Sci. USA 110, 18110–18115.

Garreaud, R.D., Aceituno, P., 2001. Interannual rainfall variability over the South American Altiplano. J. Climate 14, 2779–2789.

Garreaud, R., Vuille, M., Clement, A., 2003. The climate of the Altiplano: observed current conditions and mechanism of past changes. Palaeogeogr. Palaeoclimatol. Palaeoecol. 194 (3054), 1–18.

Garreaud, R.D., Vuille, M., Compagnucci, R., Marengo, J., 2009. Present-day South American climate. Palaeogeogr. Palaeoclimatol. Palaeoecol. 281, 180–195.

Graham, N.E., Ammann, C.M., Fleitmann, D., Cobb, K.M., Luterbacher, J., 2010. Support for global climate reorganization during the "Medieval Climate Anomaly". Clim. Dyn. 37, 1217–1245. https://doi.org/10.1007/s00382-010-0914-z.

Guyot, J.L., Molinier, M., de Oliveira, E., Cudo, K.J., Guimaraes, V., 1994. Nouveautés sur les débits monstrueux de l'Amazone. Rev. Géogr. Alp. 12, 77–83.

Guyot, J.L., Soares, L.d.M.F., 1997. Estudio de los recursos espeleólogicos de la Reserva Nacional torotoro (RNT). Formulación de una propuesta de conservación, protección y valorización. Publ. CONICOM, Cochabamba.

Haug, G.H., Hughen, K., Sigman, D.M., Peterson, L.C., Röhl, U., 2001. Southward migration of the intertropical convergence zone through the Holocene. Science 293, 1304–1308.

Hendy, C.H., 1971. Isotopic geochemistry of speleothems. 1. Calculation of effects of different modes of formation on isotopic composition of speleothems and their applicability as palaeoclimatic indicators. Geochim. Cosmochim. Acta 35, 801–824.

Herdies, D.L., da Silva, A., Silva Dias, M.A.F., Nieto Ferreira, R., 2002. Moisture budget of the bimodal pattern of the summer circulation over South America. J. Geophys. Res. 107 (D20), 8075. LBA 42-1–LBA 42-10.

Hubert, P., Carbonnel, J-P., Cchaouche, A., 1989. Segmentation des séries hydrométéorologiques. Application à des séries de précipitation et de débits de l'Afrique de l'Ouest. J. Hydrol. 110, 349–367.

Hurley, J.V., Vuille, M., Hardy, D.R., Burns, S., Thompson, L.G., 2015. Cold air incursions, δ^{18}O variability and monsoon dynamics associated with snow days at Quelccaya Ice Cap, Peru. J. Geophys. Res. 120, 7467–7487. https://doi.org/10.1002/2015JD023323.

Hurley, J.V., Vuille, M., Hardy, D.R., 2016. Forward modeling of δ^{18}O in Andean ice cores. Geophys. Res. Lett. 43 (15), 8178–8188. https://doi.org/10.1002/2016GL070150.

Insel, N., Poulsen, C.J., Sturm, C., Ehlers, T.A., 2013. Climate controls on Andean precipitation δ^{18}O interannual variability. J. Geophys. Res. 118 (17), 9721–9742. https://doi.org/10.1002/jgrd.50619.

Kanner, L.C., Burns, S.J., Cheng, H., Edwards, R.L., Vuille, M., 2013. High-resolution variability of the South American summer monsoon over the last seven millennia: insights from a speleothem record from the central Peruvian Andes. Quat. Sci. Rev. 75, 1–10.

Lavado, W., Labat, D., Ronchail, J., Espinoza, J.C., Guyot, J.L., 2012. Trends in rainfall and temperature in the Peruvian Amazon–Andes basin over the last 40 years (1965–2007). Hydrol. Process. 41, 2944–2957. https://doi.org/10.1002/hyp.9418.

Lenters, J.D., Cook, K.H., 1997. On the origin of the Bolivian High and related circulation features of the South American climate. J. Atmos. Sci. 54, 656–677.

Lenters, J.D., Cook, K.H., 1999. Summertime precipitation variability over South America: role of the large-scale circulation. Mon. Weather Rev. 127, 409–431.

Liu, X., Battisti, D.S., 2015. The influence of orbital forcing of tropical insolation on the climate and isotopic composition of precipitation in South America. J. Climate 28, 4841–4862. https://doi.org/10.1175/JCLI-D-14-00639.1.

Marengo, J.A., Liebmann, B., Grimm, A.M., Misra, V., Silva Dias, P.L., Cavalcanti, I.F.A., Carvalho, L.M.V., Berbery, E.H., Ambrizzi, T., Vera, C.S., Saulo, A.C., Nogues-Paegle, J., Zipser, E., Seth, A., Alves, L.M., 2012. Recent developments on the South American monsoon system. Int. J. Climatol. 32, 1–21.

Masson-Delmotte, V., Schulz, M., Abe-Ouchi, A., Beer, J., Ganopolski, A., González Rouco, J.F., Jansen, E., Lambeck, K., Luterbacher, J., Naish, T., Osborn, T., Otto-Bliesner, B., Quinn, T., Ramesh, R., Rojas, M., Shao, X., Timmermann, A., 2013. Information from paleoclimate archives. In: Stocker, F., Qin, D., Plattner, G.-K., Tignor, M., Allen, S.K., Boschung, J., Nauels, A., Xia, Y., Bex, V., Midgley, P.M. (Eds.), Climate Change 2013: The Physical Science Basis. Contribution of Working Group I to the Fifth Assessment Report of the Intergovernmental Panel on Climate Change. Cambridge University Press, Cambridge, United Kingdom, New York, NY, USA.

Novello, V.F., Cruz, F.W., Karmann, I., Burns, S.J., Stríkis, N.M., Vuille, M., Cheng, H., Edwards, R.L., Santos, R.V., Frigo, E., Barreto, E.A.S., 2012. Multidecadal climate variability in Brazil's Nordeste during the last 3000 years based on speleothem isotope records. Geophys. Res. Lett. 39 (23). https://doi.org/10.1029/2012GL053936.

Novello, V.F., Vuille, M., Cruz, F.W., Stríkis, N.M., De Paula, M.S., Edwards, R.L., Cheng, H., Karmann, I., Jaqueto, F.P., Trindade, R.I.F., Hartman, G.A., Moquet, J.S., 2016. Centennial-scale solar forcing of the South American Monsoon System recorded in stalagmites. Sci. Rep., 1–8. https://doi.org/10.1038/srep24762.

Oppo, D.W., Rosenthal, Y., Linsley, B.K., 2009. 2,000-year-long temperature and hydrology reconstructions from the Indo-Pacific warm pool. Nature 460 (7259). https://doi.org/10.1038/nature08233. 1113–6.

Perez, L., García-Rodríguez, F., Hanebuth, T.J.J., 2016. Variability in terrigenous sediment supply offshore of the Río de la Plata (Uruguay) recording the continental climatic history over the past 1200 years. Clim. Past 12, 623–634. https://doi.org/10.5194/cp-12-623-2016.

Piovano, E.L., Ariztegui, D., Cordoba, F., Cioccale, J., Sylvestre, F., 2009. Hydrological variability in South America below the tropic of Capricorn (Pampas and Patagonia, Argentina) during the Last 13.0 Ka. In: Vimeux, F., Sylvestre, F., Khodri, M. (Eds.), Past Climate Variability in South America and Surrounding Regions, from the Last Glacial Maximum to the Holocene. Springer, pp. 323–352.

Reuter, J., Stott, L., Khider, D., Sinha, A., Cheng, H., Edwards, R.L., 2009. A new perspective on the hydroclimate variability in northern South America during the Little Ice Age. Geophys. Res. Lett. 36, L21706. https://doi.org/10.1029/2009GL041051.

Ronchail, J., Bourrel, L., Cochonneau, G., Vauchel, P., Phillips, L., Castro, A., Guyot, J., De Oliveira, E., 2005. Inundations in the Mamore basin (South-Western Amazon–Bolivia) and sea-surface temperature in the Pacific and Atlantic Oceans. J. Hydrol. 302, 223–238.

Samuels-Crow, K.E., Galewsky, J., Hardy, D.R., Sharp, Z.D., Worden, J., Braun, C., 2014. Upwind convective influences on the isotopic composition of atmospheric water vapor over the tropical Andes. J. Geophys. Res., Atmos. 119, 7051–7063.

Satyamurty, P., da Costa, C.P.W., Manzi, A.O., 2013. Moisture source for the Amazon basin: a study of contrasting years. Theor. Appl. Climatol. 111, 195–209.

Schulz, M., Mudelsee, M., 2002. REDFIT: estimating red-noise spectra directly from unevenly spaced paleoclimatic time series. Comput. Geosci. 28, 421–426.

Segura, H., Espinoza, J.C., Junquas, C., Takahashi, K., 2016. Evidencing decadal and interdecadal hydroclimatic variability over the Central Andes. Environ. Res. Lett. 11, 094016. https://doi.org/10.1088/1748-9326/11/9/094016.

Sturm, C., Vimeux, F., Krinner, G., 2008. Intraseasonal variability in South America recorded in stable water isotopes. J. Geophys. Res. 112. https://doi.org/10.1029/2006JD008298.

Sulca, J., Vuille, M., Silva, Y., Takahashi, K., 2016. Teleconnections between the Peruvian central Andes and Northeast Brazil during extreme rainfall events in austral summer. J. Hydrometeorol. 17, 499–515.

Tapia, P.M., Fritz, S.C., Baker, P.A., Seltzer, G.O., Dunbar, R.B., 2003. A late Quaternary diatom record of tropical climate history from Lake Titicaca (Peru and Bolivia). Palaeogeogr. Palaeoclimatol. Palaeoecol. 194 (1), 139–164.

Thompson, L.G., Mosley-Thompson, E., Davis, M.E., Zagorodnov, V.S., Howat, I.M., Mikhalenko, V.N., Lin, P.N., 2013. Annually resolved ice core records of tropi-

cal climate variability over the past ~1800 years. Science 340. https://doi.org/10.1126/science.1234210. 945–50.

Torrence, C., Compo, G.P., 1998. A practical guide to wavelet analysis. Bull. Am. Meteorol. Soc. 79, 61–78.

Vera, C., Higgins, W., Amador, J., Ambrizzi, T., Garreaud, R., Gochin, D., Gutzler, D., Lettenmaier, D., Marengo, J., Mechoso, C., Nogues-Paegle, J., Silva Diaz, P.-L., Zhang, C., 2006. Towards a unified view of the American Monsoon System. J. Climate 19, 4977–5000.

Vimeux, F., Gallaire, R., Bony, S., Hoffmann, G., Chiang, J.C.H., 2005. What are the climate controls on dD in precipitation in the Zongo Valley (Bolivia)? Implications for the Illimani ice core interpretation. Earth Planet. Sci. Lett. 240, 205–220.

Vuille, M., 1999. Atmospheric circulation over the Bolivian Altiplano during dry and wet periods and extreme phases of the Southern Oscillation. Int. J. Climatol. 19, 1579–1600.

Vuille, M., Bradley, R.S., Keimig, F., 2000. Interannual climate variability in the central Andes and its relation to tropical Pacific and Atlantic forcing. J. Geophys. Res. 105, 12447–12460.

Vuille, M., Keimig, F., 2004. Interannual variability of summertime convective cloudiness and precipitation in the central Andes derived from ISCCP-B3 data. J. Climate 17, 3334–3348.

Vuille, M., Werner, M., 2005. Stable isotopes in precipitation recording South American summer monsoon and ENSO variability – observations and model results. Clim. Dyn. 25, 401–413. https://doi.org/10.1007/s00382-005-0049-9.

Vuille, M., Burns, S.J., Taylor, B.L., Cruz, F.W., Bird, B.W., Abbott, M.B., Kanner, L.C., Cheng, H., Novello, V.F., 2012. A review of the South American monsoon history as recorded in stable isotopic proxies over the past two millennia. Clim. Past 8, 1309–1321. https://doi.org/10.5194/cp-8-1309-2012.

Yoon, J.-H., Zeng, N., 2010. An Atlantic influence on Amazon rainfall. Clim. Dyn. 34, 249–264. https://doi.org/10.1007/s00382-009-05516.

Zhou, J., Lau, K., 1998. Does a monsoon climate exist over South America? J. Climate 11, 1020–1040.